0026-895X/97/020250-12$3.00/0

MOLECULAR PHARMACOLOGY, **51:**250–261 (1997).

Structural and Functional Characterization of the Human α3 Nicotinic Subunit Gene Promoter

DIEGO FORNASARI, ELENA BATTAGLIOLI, ADRIANO FLORA, SUSANNA TERZANO, and FRANCESCO CLEMENTI

CNR Cellular and Molecular Pharmacology Center, Department of Medical Pharmacology, University of Milan, 20129 Milan, Italy

Received July 8, 1996; Accepted October 25, 1996

SUMMARY

We describe the structural and functional features of the human α3 nicotinic receptor subunit promoter. A 0.35-kb region immediately upstream of the start codon was identified that when transfected in human neuroblastoma cells was able to drive the expression of the luciferase reporter gene with a strength comparable to that of the well-characterized simian virus 40 promoter/enhancer. This region displayed the features of a multi-start-site, GC-rich, TATA-less, and CAAT-less promoter, containing many overlapping Sp1 and AP-2 putative binding sites. Further dissections of the 0.35-kb fragment revealed that its 3′ region, specifying the 5′ UT of the mRNA, plays a relevant positive effect in determining the strength of the promoter. This region contains putative *cis*-acting elements for AP-2, nuclear factor-κB, and the recently described multiple-start site element downstream-1. By mutation analysis, we showed that these sites are functional and when combined increase the promoter activity by 4-fold. The 0.35-kb promoter was found to be under the negative control of upstream sequences that include a modern Alu repeat. The α3 Alu repeat works as a composite region, containing both positive and negative elements that control the activity of the downstream promoter. Finally, we investigated the tissue-specific activity of the human α3 gene 5′ regulatory sequences, showing that they are able to drive the expression of the reporter gene preferentially in neuronal cells.

Nicotinic acetylcholine receptors are ligand-gated ion channels expressed at the neuromuscular junction, in autonomic ganglia, and in several areas of the vertebrate CNS. They are also present on adrenal chromaffin cells, where they control the release of catecholamines. Like their muscular counterpart, neuronal-type nicotinic receptors have a pentameric stoichiometry and are composed of ligand-binding and structural subunits, which are encoded by a large family of genes homologous to those encoding the muscle isoforms. Recombinant DNA technology and heterologous expression in *Xenopus laevis* oocytes have resulted in the identification of eight ligand-binding subunits (α2-9) and three structural subunits (β2-4) that can combine to form different receptor subtypes with distinctive pharmacological and electrophysiological properties. More precisely, some agonist-binding subunits (α7-9) have been shown to work as homo-oligomeric channels, whereas α2-4 isoforms must be coexpressed with at least one structural subunit to generate functional molecules (for reviews, see Refs. 1 and 2). *In vivo*, the structure of native receptors is likely to be more complex, with the possibility that more than one type of agonist binding and/or structural subunit assembles into the same receptor molecule with multiple stoichiometries (2, 3). It implies that a stringent qualitative and quantitative control on the expression of each subunit must be exerted to generate specific receptor subtypes with different functions in synaptic pathways. *In situ* hybridization and immunocytochemical studies corroborate this idea, demonstrating that certain subunits are preferentially or exclusively expressed in the CNS or in autonomic ganglia; in the former case, the expression can be restricted to very few brain structures (4, 5).

The regional distribution pattern of each subunit seems to be under the control of fine regulatory mechanisms that start to operate early during development; the expression of some subunits is often precocious and sometimes coincides with the early events of neuronal differentiation. Interestingly, some nicotinic isoforms are transiently present in certain neural structures, disappearing during the perinatal period (5). Although the the majority of the anatomic organization of the neuronal cholinergic-nicotinic system seems to be defined during ontogenesis, the expression levels of certain subunits undergo important modifications in postnatal life, as in those areas of the CNS that show structural rearrangement and progressive neurochemical maturation during the first 21 days after birth (6).

This work was supported in part by Fabriques de Tabac Reunies (Neuchotel, Switzerland).

ABBREVIATIONS: CNS, central nervous system; SV40, simian virus 40; MED-1, multiple-start site element downstream-1; UT, untranslated; GAPDH, glyceraldehyde-3-phosphate dehydrogenase; RSV, Rous sarcoma virus; NFκB, nuclear factor-κB; NRSE, neuron-restrictive silencer element.

These highly regulated spatial and temporal expression patterns are likely to rely on sophisticated genetic mechanisms that can be partially approached through the characterization of the regulatory sequences that control the transcription of the different neuronal nicotinic subunit genes. Although information for some chicken and rat genes is available (7–15), studies on the human genes have not been performed. In the current study, we describe for the first time a human promoter controlling the expression of the α3 nicotinic subunit gene.[1]

Several lines of evidence have demonstrated that autonomic ganglia are not simply relay stations but rather display a high degree of integrative activity. In light of the relevant role of the α3 nicotinic subunit in ganglionic transmission (1, 2), the comprehension of the mechanisms that govern its transcription may also help to obtain new insights into the functions of the autonomic nervous system, especially concerning adaptive responses to environmental cues.

Materials and Methods

Isolation of the 5′-flanking region of the human α3 nicotinic subunit gene. The genomic clone λc16, which has been previously shown to contain coding sequences of both β4 and α3 genes (16), was digested with *Apa*I and analyzed by Southern blotting. A 5.1-kb *Apa*I fragment was recognized by both an *Apa*I/*Eco*RI cDNA probe, corresponding to part of the 3′ UT of the β4 subunit (17), and an *Eco*RI/*Nco*I cDNA probe, corresponding to the 5′ UT of the α3 subunit (18). This fragment was purified, ligated into the *Apa*I site of pBluescript II KS$^+$ (Stratagene, La Jolla, CA), and characterized by restriction analysis and sequencing (TAQuence, version 2.0; United States Biochemical, Cleveland, OH).

RNA preparation. Total RNA were isolated from different cell lines by the use of RNAfast-II (Molecular Systems, San Diego, CA) according to the manufacturer's instructions. Briefly, ~10^8 cells were collected by centrifugation and lysed with a solution containing guanidine salts and phenol. RNA was extracted with chloroform and purified on the RNA-binding resin. Poly(A)$^+$ mRNA was prepared with Oligotex-dT (Qiagen, Studio City, CA) according to the manufacturer's instructions, with minor modifications. Total and polyadenylate RNAs were quantified with spectrophotometry.

RNase protection analysis. A 201-bp fragment encoding part of the cytoplasmic domain of the human α3 nicotinic subunit (nucleotides 976-1176 according to Ref. 18) and a 338-bp *Bgl*II/*Sfi*I fragment, corresponding to the region immediately upstream of the α3 start codon (Fig. 1) were subcloned in pBluescript II KS$^+$. On linearization with appropriate restriction enzymes, constructs were transcribed *in vitro* by the use of T3 or T7 polymerase (MAXIscript; Ambion, Austin, TX) to obtain [α-^{32}P]UTP-labeled antisense RNA. Because of the presence of part of the pBluescript II KS$^+$ polylinker, the full-length riboprobes were 262 and 391 bp. A 316-bp fragment of the human *GAPDH* gene (pTRI-GAPDH-human antisense control template; Ambion), *in vitro* transcribed by T7 polymerase, was used to check the quality of the different RNAs. The full length riboprobe was 404 bp, including part of the vector polylinker. The full-length RNA probes were purified from 6% acrylamide gels containing 8 M urea. RNase protection assays were carried out with the RPA II kit (Ambion) with some modifications. The 262- and 391-bp purified RNA probes were hybridized overnight with 3 μg of poly(A)$^+$ at 42° and 60°, respectively. The *GAPDH* RNA probe was hybridized overnight with 0.5 μg of poly(A)$^+$ at 42°. Single-stranded RNA was digested with 5 units/ml RNase A and 200 units/ml RNase T_1 for 1 hr. Yeast RNA (10 μg) was used instead of cellular RNA as a negative control. The products of the RNase protection assay were analyzed on 6% acrylamide gels containing 8 M urea. DNA sequence ladders were used as molecular weight markers.

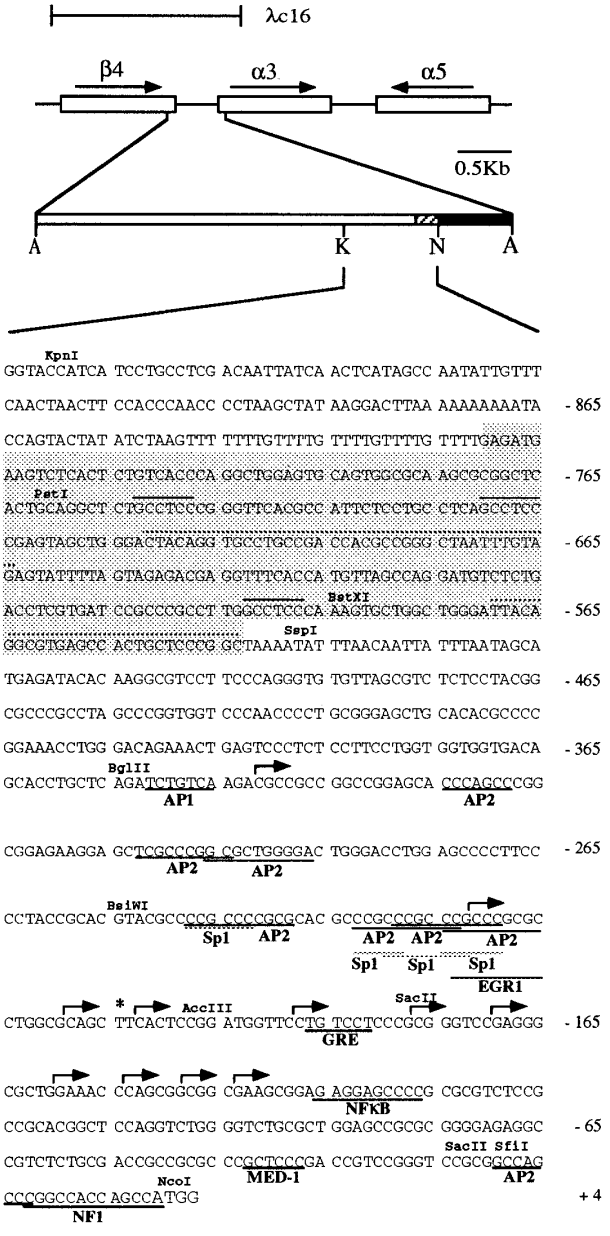

Fig. 1. Human genomic cluster containing the three nicotinic subunits (β4, α3, and α5) and nucleotide sequence of the 1-kb *Kpn*I/*Nco*I fragment corresponding to the 5′-flanking region of the human α3 gene. *Line at the top*, gene segment contained in the λc16 phage clone. *Arrows in the genomic cluster*, direction of transcription; *enlargement below,* 5.1-kb cloned region between β4 and α3 plus some restriction sites (*A*, *Apa*I; *K*, *Kpn*I; *N*, *Nco*I); *striped region*, 5′ UT of the cloned α3 cDNA in the 5.1-kb fragment; *filled region*, part of the coding region of the human α3 gene in the 5.1-kb fragment. The nucleotide sequence of the *Kpn*I/*Nco*I fragment is shown: positions are numbered from the initiator codon. *Arrows*, transcriptional start sites identified by RNase Protection (see legend to Fig. 3); *, First nucleotide at the 5′ end, previously identified by cDNA cloning. Relevant restriction sites used for subcloning and putative DNA binding sites for the indicated transcription factors are shown. *Shaded region*, Alu sequence; *overlined*, Alu core repeats; *superscript dashes*, reducer sequences; AP1, activator protein-1; AP-2, activator protein-2; EGR1, ▮; GRE, glucocorticoid response element.

Construction of human α3 promoter-luciferase fusion plasmids. All restriction enzymes were purchased from Promega (Mad-

[1] Accession no. Y09146 in the EMBL nucleotide sequence database

ison, WI). Different segments of the 5′-flanking region of human α3 were subcloned into the pGL3-basic vector (Promega), upstream of the luciferase reporter gene (Figs. 1 and 4–6). When not differently identified, the constructs are named with a number, identifying the length of the subcloned fragment, followed by the letters indicating the restriction sites into which they were ligated (K = *Kpn*I, B = *Bgl*II, W = *Bsi*WI, A = *Acc*III, N = *Nco*I, S = *Sac*II, P = *Pst*I, and X = *Bst*XI). The 4.3 KN construct was generated as follows: the 5.1-kb *Apa*I fragment in pBluescript II KS$^+$ was separately digested with *Nco*I and *Kpn*I or *Kpn*I alone. The digestions resulted in the excision of a 1-kb *Kpn*I/*Nco*I fragment and a 3.3-kb *Kpn*I fragment that was generated because of the presence of a *Kpn*I site in the polylinker of pBluescript II KS$^+$, immediately upstream of the *Apa*I site. The two inserts were gel purified by the use of Qiaex (Qiagen) and ligated by three-way ligation into the *Nco*I and *Kpn*I sites of pGL3-basic. The correct orientation and the identity of the two inserts were verified by restriction analysis and DNA sequencing. The resulting construct, 4.3 KN, contains the 3′ UT of β4, the 5′ UT of α3, and the intervening region (Fig. 1). 5′ and 3′ deletions (Fig. 4) of this construct were obtained as follows: 1 KN was generated by digestion of the 4.3 KN plasmid with *Kpn*I, followed by religation; and the 0.35 BN construct was obtained by subcloning the purified 0.35-kb *Bgl*II/*Nco*I fragment into the corresponding restriction sites of pGL3-basic. The 0.2 AN plasmid was obtained by subcloning the purified *Acc*III/*Nco*I fragment into the *Xma*I and *Nco*I sites of pGL3. The constructs used to investigate the functional role of the Alu sequence were obtained as follows: the 0.8 PN derives from the 1 KN plasmid on digestion with *Kpn*I and *Pst*I; after gel purification, the extremities were blunted by T4 DNA polymerase and religated by T4 DNA ligase. ΔAlu derives from the 1 KN plasmid, which was digested with *Pst*I and *Bst*XI, gel purified, blunt ended, and religated. The 0.6 XN construct again derives from the 1 KN plasmid, digested with *Kpn*I and *Bst*XI, gel purified, blunt ended, and religated. The 0.6Δr (r = reducer) represents a 30-bp 5′ deletion of the previous construct that was obtained by digesting the 0.6 XN plasmid with *Ssp*I. A band of 4.5 kb was gel purified and digested with *Nco*I; after gel purification, the resulting *Ssp*I/*Nco*I fragment was cloned into the *Sma*I and *Nco*I sites of pGL3-basic. Notably, in this set of constructs, the 5′ UT of the luciferase was removed, and the coding region of the reporter gene was directly fused to the 5′ UT of the α3 nicotinic subunit at the *Nco*I site. The natural context for initiation of translation was not affected in these constructs. The 0.16 BA construct was obtained by digestion of the 0.35 BN plasmid with *Acc*III and *Xma*I; the purified *Xma*I/*Acc*III fragment was then subcloned into the *Xma*I/*Sma*I site of pGL3 basic, in appropriate orientation. The 3.3 K and 0.6 KB constructs were generated by subcloning the purified fragments into the polylinker of pGL3-basic. The plasmids derived from the 0.35 KN construct, bearing mutations in the 3′ end of the promoter, were obtained as follows: ΔNF-1 was generated by replacing the *Sfi*I/*Nco*I fragment with a double-strand oligonucleotide bearing two point mutations in the NF-1 site. ΔAP-2 contains a 3-bp deletion in the downstream AP-2 sequence, obtained through *Sfi*I digestion, followed by removal of the overhangs and religation. Δ*Sac*II contains a deletion of the 150-bp *Sac*II fragment. ΔNFκB contains a 4-bp deletion in the NFκB sequence; the mutation was created in the *Sac*II fragment and subcloned in a derivative of pGEM-5Z (Promega), which lacks *Ban*II restriction sites. The plasmid was digested with *Ban*II, blunt ended, and religated. The mutated *Sac*II fragment was subcloned in Δ*Sac*II, in the appropriate orientation. ΔMED-1 contains a 4-bp mutation in the 6-bp consensus sequence of MED-1. The 250-bp *Sac*I/*Bsi*EI fragment contained in the 0.35-kb promoter was gel purified. A double-strand oligonucleotide, corresponding to the 32-bp *Bsi*EI/*Sac*II region of the promoter, was generated bearing the MED-1 mutation. The oligonucleotide and the 250-bp fragment were cloned in pBluescript II KS$^+$ by three-way ligation. The *Sac*II fragment was gel purified and subcloned in Δ*Sac*II plasmid. ΔAP-2-ΔNFκB was obtained from ΔNFκB by applying the same procedures used to obtain ΔAP-2. ΔAP-2-Δ*Sac*II was obtained from ΔAP-2 by removing the *Sac*II fragment. pGL3 control + 0.2 kb was generated as follows: pGL3 control was digested with *Hin*dIII, blunt ended by T4 DNA Pol, and digested again with *Nco*I to remove the DNA region specifying the 5′ UT of the luciferase gene. The 0.2 AN was digested with *Nhe*I, blunt ended, and digested again with *Nco*I to excide the 0.2 *Acc*III/*Nco*I fragment. The fragment was gel purified and ligated blunt/*Nco*I in the pGL3 control plasmid previously prepared as described. All mutations were confirmed by DNA sequencing. The RSV-β-galactosidase plasmid, used to normalize for transfection efficiency, was obtained from pGL3-basic by replacing the luciferase gene with the β-galactosidase gene, derived from pNASS (Clontech, Palo Alto, CA). The RSV promoter was obtained from pRc/RSV (InVitrogen, San Diego. CA) and subcloned into the polylinker of pGL3-basic, upstream of the reporter gene.

Cell lines and cultures. The human neuroblastoma cell lines SY5Y and SK-N-BE and the human rhabdomyosarcoma cell line TE671 (CRL-8805, American Type Culture Collection, Rockville, MD) were grown in RPMI 1640, 10% fetal calf serum, 50 units/ml penicillin, 50 mg/ml streptomycin, and 2 mM L-glutamine. HeLa cells were grown in Dulbecco's modified Eagle's medium, 10% fetal calf serum, 50 units/ml penicillin, 50 mg/ml streptomycin, 2 mM L-glutamine, and 110 μg/ml sodium pyruvate.

Transient transfections. Plasmid DNA was purified with Qiagen columns and transfected into logarithmically growing cells using a Gene Pulser electroporator (BioRad, Hercules, CA).

Cells were washed twice with phosphate-buffered saline, harvested, and resuspended in their own medium without fetal calf serum. For each transfection, we used 4×10^6 cells in 0.8 ml of medium. Equimolar amounts of different constructs were used, with 20 μg for the shortest plasmid, pGL3-basic. In each experiment, 5 μg of RSV-β-galactosidase plasmid was cotransfected to normalize for transfection efficiency. The pGL3 control plasmid (Promega), which contains the SV40 promoter and enhancer and the promoterless pGL3-basic (Promega), were always used in parallel transfections as positive and negative controls. Cells were incubated with DNA for 10 min on ice and then shocked, using the following parameters: 960 μF and 280 V for SY5Y cells, 960 μF and 270 V for SK-N-BE and TE671 cells, and 960 μF and 200 V for HeLa cells. Cells were placed on ice for 10 min, transferred to 25 ml of prewarmed media, and harvested after 48 hr for luciferase and β-galactosidase assays.

All transfections were performed in triplicate, and each construct was tested in at least three independent experiments using different batches of plasmid preparations.

Luciferase and β-galactosidase assays. Cells were harvested, washed twice in phosphate-buffered saline, and lysed in the Reporter Lysis Buffer (Promega) for 15 min at room temperature. After a brief centrifugation to remove cellular debris, 10 μg of cellular extract in a final volume of 20 μl was added to 100 μl of Luciferase Assay Reaction (Promega) and tested for luciferase activity with a Berthold Lumat LB 9501 luminometer for 60 sec. In parallel, 10 μg of the same extracts were processed for β-galactosidase expression by using the Luminescent β-Galactosidase Detection Kit (Clontech), following the supplied protocol. Samples were previously heat treated at 50° for 1 hr to destroy any endogenous β-galactosidase activity. This treatment does not affect the bacterial β-galactosidase expressed by the RSV-β-Gal plasmid (19); this procedure was also verified for each cell line that we used in our laboratory. β-Galactosidase activity was determined with the luminometer for 5 sec. In both luciferase and β-galactosidase assays, the background activities, which were measured in the absence of cellular extract, were subtracted. The protein content of the cellular extracts was measured with a BCA Protein Assay (Pierce Chemical, Rockford, IL).

Analysis of the data obtained by transient transfections. For each construct, the values of luciferase (expressed as relative luminescent units) that were obtained in the different experiments were plotted versus the corresponding values of β-galactosidase (also expressed as relative luminescent units). Linear correlations were obtained with correlation coefficients ranging from 0.75 and 0.99.

The transcriptional activity of each construct was defined as the slope of the straight line and was expressed as fold increase over the transcriptional activity of the promoterless plasmid pGL3-basic. The statistical significance of the differences in the transcriptional activities among constructs was assessed by analysis of variance ($F < 0.05$).

Computer-assisted analysis. The presence of putative transcription factor binding sites (Fig. 1) was evaluated with the MacPattern program (Macintosh) in conjunction with the EMBL Transcription Factor Database. Statistical analysis was carried with StatWorks software (Macintosh).

Results

Isolation of the 5′-flanking region of the human α3 nicotinic subunit gene. The human β4, α3, and α5 nicotinic subunit genes are located on chromosome 15, forming a genomic cluster that is conserved across species (Fig. 1). The genomic clone λc16, which has been shown to contain coding sequences of both β4 and α3 genes (16), was analyzed by restriction digestions, followed by Southern blotting and hybridization to specific probes. λc16 contains a 5.1-kb *Apa*I fragment that was recognized by two cDNA probes corresponding to the 3′ UT of the β4 subunit and the 5′ UT of the α3 subunit (data not shown); this result indicated that the entire genomic region between the β4 and α3 genes was contained in the *Apa*I/*Apa*I fragment. The cDNA sequencing of the human α3 subunit has been demonstrated to contain the ATG start codon in an *Nco*I site (18). After a preliminary restriction analysis, a 1-kb *Kpn*I/*Nco*I fragment was purified from the 5.1-kb *Apa*I fragment (Fig. 1), subcloned into the pGL3-basic vector. and sequenced through the use of GL-primer 2 (Promega). This genomic fragment overlapped the 5′ UT of the α3 cDNA by 201 bp (Fig. 1). A 3.3-kb *Apa*I/*Kpn*I fragment and a 0.8-kb *Nco*I/*Apa*I fragment located upstream and downstream of the 1-kb *Kpn*I/*Nco*I segment, respectively, were also characterized by DNA sequencing and proved to contain the 3′ UT of the β4 subunit and part of the coding region of α3 subunit gene, including the signal peptide encoding sequence, respectively. These results confirmed that the *Apa*I fragment contained the whole genomic region located between the β4 stop codon and the α3 start codon. The entire sequence of the 1-kb *Kpn*I/*Nco*I fragment, which was likely to contain the α3 gene promoter, was determined (Fig. 1). The results of the sequence analysis revealed that the 1-kb *Kpn*I/*Nco*I fragment can be divided by the *Bgl*II restriction site into two subregions with different nucleotide composition: a 0.35-kb *Bgl*II/*Nco*I segment, proximal to the start codon, which is very rich in GC (75%), and a 0.6-kb *Kpn*I/*Bgl*II upstream segment with a 52% GC content. The latter subregion contains an Alu repeat that displays 85% identity with a canonical Alu sequence (Fig. 1).

Detection of α3 transcripts in human neuroblastoma cell lines by RNase protection assay. To verify that SY5Y and SK-N-BE human neuroblastoma cell lines expressed α3 transcripts in our culture conditions, we carried out an RNase protection assay (Fig. 2A). We used a cRNA antisense probe, complementary to part of the region coding for the cytoplasmic domain of α3, which is the least conserved part among the different subunits of the nicotinic receptor family. A protected band of the expected size was detected in neuroblastoma cell lines and was prominent in SY5Y cells. A much less intense band, a few nucleotides shorter, was also detected and was probably the result of RNase "nibbling." The negative control in which yeast RNA was substituted for cellular RNA revealed no bands. No signals were detected in the non-neuronal cell lines, indicating that at least in HeLa and TE671 cells, the tissue specificity of the α3 expression is conserved even in tissue culture conditions. The same RNA preparations from the four cell lines were also tested by using a GAPDH probe (Fig. 2B). A strong band, with the correct size and the same intensity, was obtained in all RNA samples

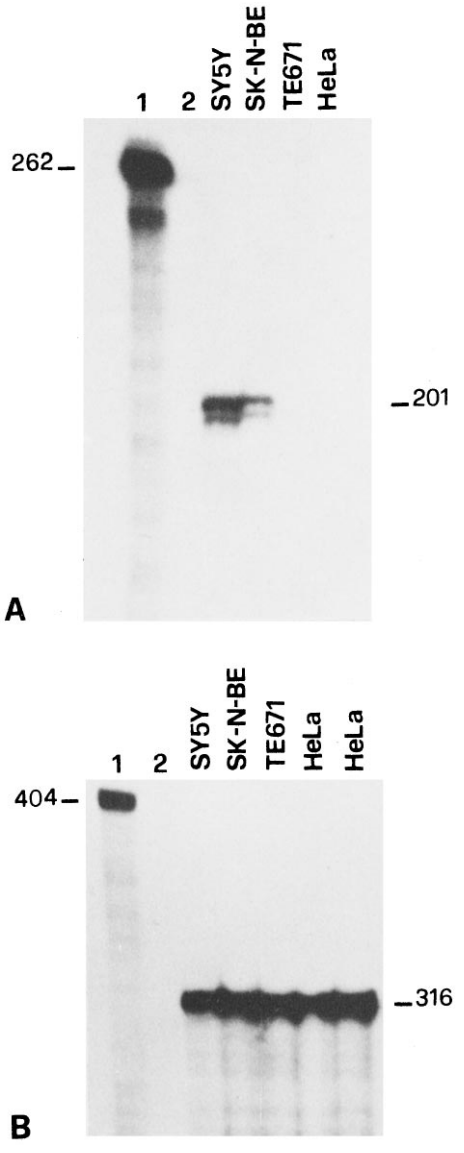

Fig. 2. Expression of the human α3 mRNA in neuronal (SY-5Y and SK-N-BE) and non-neuronal cell lines (HeLa, TE671). A, A 262-bp [α-^{32}P]UTP-labeled antisense riboprobe corresponding to 201 bp of the region encoding part of the cytoplasmic domain of human α3 nicotinic subunit and to 61 bp of the pBluescript II KS$^+$ polylinker was hybridized to mRNA purified from the indicated cell lines. *1 and 2*, undigested probe and negative control, respectively, in which the probe was incubated with yeast RNA and then digested with RNases. B, A 404-bp [α-^{32}P]UTP-labeled antisense riboprobe corresponding to 316 bp of the ubiquitous gene GAPDH and to 88 bp of the vector polylinker was hybridized to the same mRNA preparations used in A. *1 and 2*, undigested probe and negative control, respectively, in which the probe was incubated with yeast RNA and then digested with RNases. *Numbers on the left*, size of the full-length antisense riboprobes; *numbers on the right*, size of the protected bands.

but not in the negative controls, confirming that the differences in the α3 expression between neuronal and non-neuronal cell lines were not due to RNA degradation.

Mapping of the transcription start sites of the human α3 nicotinic subunit. To map the 5′ termini of the human α3 mRNA, we carried out an RNase protection assay by using as probe a 338-bp *Bgl*II/*Sfi*I fragment that at its 3′ end overlaps with the 5′ UT of the α3 cDNA (Fig. 1). Several transcription start points were identified in the two neuronal cell lines, with different preferential use (Fig. 3). No bands were detected in the negative control or in the non-neuronal cell line RNA. All of the transcription start sites except one were clustered in a region of ~80 bp, which is almost completely overlapping the 5′ UT of the α3 cDNA (Fig. 1). The origin of the −341 transcription start site (Figs. 3 and 1), which is prominent in SK-N-BE cells, is unclear. Its presence has been also confirmed by using a 280-bp *Ssp*I/*Bsi*WI riboprobe (Fig. 1 and data not shown), and an investigation of whether it reflects the existence of an additional upstream promoter is under way.

Functional delineation of the human α3 nicotinic subunit gene promoter. To localize the region necessary and sufficient for promoter activity, we generated chimeric constructs containing different genomic fragments of the 5′-flanking region of the human α3 nicotinic subunit gene fused to the luciferase reporter gene. Because both the ATG start codons of the human α3 subunit and the luciferase reporter gene are embedded in an *Nco*I restriction site, we were able to generate chimeric constructs in which different segments of the 5′ regulatory region were directly fused to the luciferase coding sequence. The different constructs were transfected into the human neuroblastoma cell lines SY5Y and SK-N-BE along with an RSV-β-galactosidase plasmid as internal control for transfection efficiency. After 48 hr, luciferase and β-galactosidase activities were measured. Similar but not identical results were obtained in the two cell lines (Fig. 4). In both neuroblastomas, the 4.3 KN construct, containing the whole intergenic region between β4 and α3, displayed a consistent promoter activity, 20 times over the background, evaluated as the luciferase expression driven by the promoterless pGL3 basic plasmid and 40% of the activity of pGL3 control, which contains the well-characterized SV40 promoter/enhancer. When a 5′ deletion of 3.3 kb was carried out, the resulting 1 KN plasmid showed a 50% decrease in the expression of the reporter gene only in SY5Y cells, whereas its transcriptional activity did not change in SK-N-BE cells. The 3.3-kb *Kpn*I deleted fragment displayed negligible activity when tested alone. The 1 KN construct was further dissected by removal of the 0.6-kb *Kpn*I/*Bgl*II 5′ region to generate the 0.35 BN plasmid. The promoter strength of this construct was as much as 3.5 times more than that of the 1 KN construct in both cell lines, indicating the presence of a negative element in the 0.6-kb deleted region. The 0.6 KB construct showed only basal activity.

The 0.35-kb *Bgl*II/*Nco*I fragment contains the DNA region specifying the 5′ UT of the mRNA (Fig. 1), as demonstrated by cDNA cloning and RNase protection assay. To understand whether this region could play a role in gene expression, we generated the 0.16 BA construct. This plasmid represents a 3′ deletion of the 0.35 BN plasmid, lacking most of the DNA segment specifying the 5′ UT of α3 subunit and containing the DNA specifying the 5′ UT of the luciferase reporter gene,

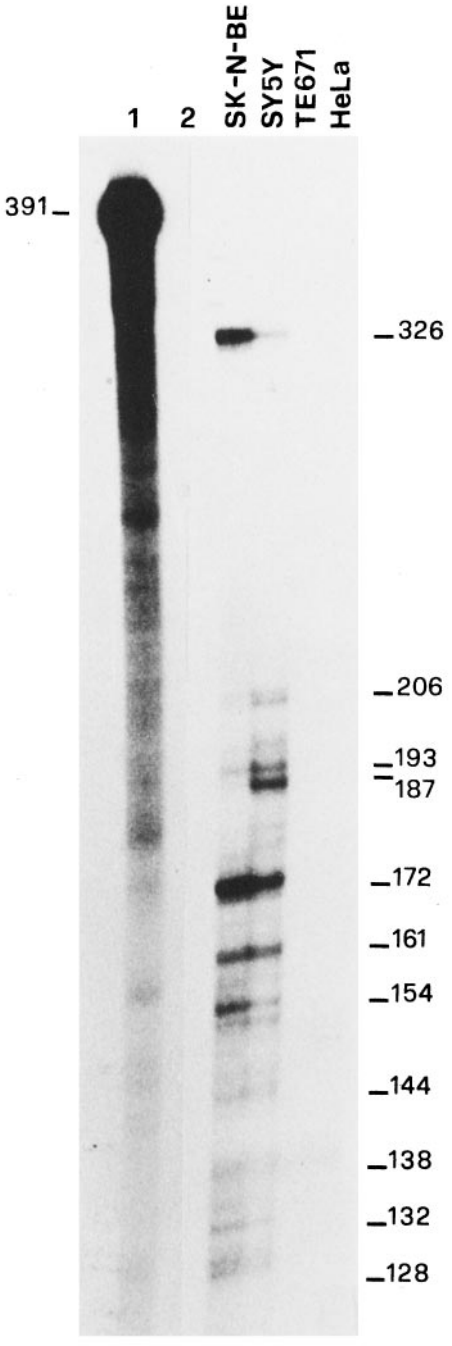

Fig. 3. Mapping of the transcription start sites of the human α3 nicotinic subunit. A 391-bp [α-^{32}P]UTP-labeled antisense riboprobe corresponding to the 326-bp *Bgl*II/*Sfi*I fragment of the 5′-flanking region (see Fig. 2) and to 65 bp of the pBluescript II KS$^+$ polylinker was hybridized to mRNA purified from the indicated cell lines. *Numbers on the right*, size of the different protected bands; *number on the left*, full-length antisense riboprobe. *1 and 2*, undigested probe and negative control, respectively, in which the probe was incubated with yeast RNA and then digested with RNases.

which is 90 bp. Importantly, both the 0.35 BN and the 0.16 BA constructs contained the luciferase gene in an optimal context for translation initiation (20). On transfection, the 3′ deleted construct displayed a four times weaker promoter strength than the parental plasmid, whereas the 0.2 AN construct, containing only the α3 5′UT specifying region, showed no transcriptional activity itself.

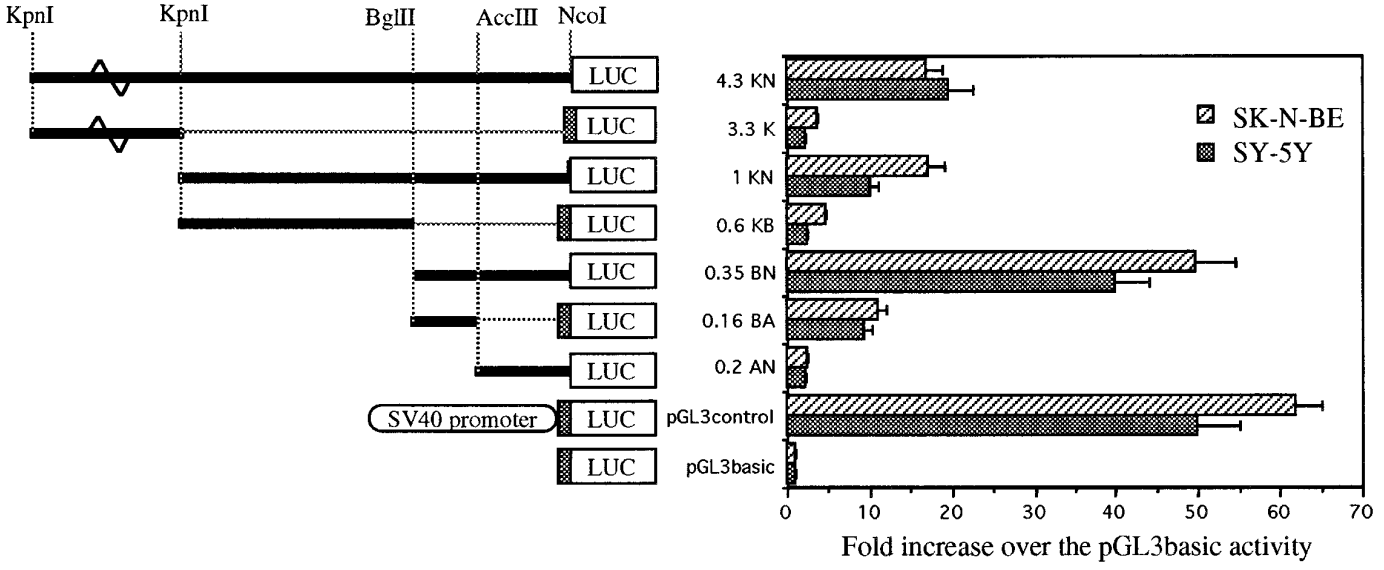

Fig. 4. Functional delineation of the human α3 nicotinic subunit gene promoter in SY5Y and SK-N-BE human neuroblastoma cell lines. *Left*, chimeric constructs, in which different parts of the α3 5′ regulatory region are fused to the luciferase (*LUC*) reporter gene. Note that the 3.3-kb *Kpn*I fragment is not to scale. *Open box*, luciferase gene coding region; *shaded portion of box*, DNA region specifying the 5′ UT of the luciferase. Note that this region, which is 90 bp, is not to scale. In the other constructs, the entire DNA region specifying the 5′ UT of the α3 mRNA was directly fused to the coding sequence of the reporter gene. In the pGL3 control plasmid, the SV40 enhancer is located downstream of the luciferase gene and is not indicated. *Bars*, transcriptional activity of the construct calculated as described in Materials and Methods and expressed as fold increase over the transcriptional activity of the promoterless plasmid pGL3-basic. The standard deviation is indicated. Each construct was tested at least three times in triplicate with two independent plasmid preparations.

To summarize, the 0.35-kb *Bgl*II/*Nco*I fragment is able to drive the expression of the luciferase reporter gene with a strength comparable to that of a viral promoter in both neuroblastoma cell lines. This promoter is negatively regulated by the 0.6-kb *Kpn*I/*Bgl*II upstream region and requires the presence of the 3′ DNA segment specifying the 5′ UT of the α3 subunit for full activity.

The 0.35-kb *Bgl*II/*Nco*I fragment contains all of the transcription start points identified by RNase protection. Computer-assisted analysis indicated that this region resembles a GC-rich (75%) TATA-less and CAAT-less promoter, with several Sp1 binding sites, upstream of the cluster of transcription start points. Several AP-2 binding sites were also identified along with single early growth response gene 1 NFκB, NF-1, activator protein-1, MED-1, and glucocorticoid response element putative *cis*-acting elements (Fig. 1).

Functional characterization of the *Acc*III/*Nco*I region specifying the 5′ UT of the α3 mRNA. Our data indicated that the *Acc*III/*Nco*I fragment, corresponding to the 3′ end of the *Bgl*II/*Nco*I α3 promoter region and specifying most of the 5′ UT of the α3 mRNA, had a relevant positive effect on gene expression. To test whether this DNA region could also exert its function in conjunction with an heterologous promoter, we engineered pGL3 control plasmid, which contains the SV40 promoter/enhancer, by replacing the DNA region specifying the 5′ UT of the luciferase gene with the *Acc*III/*Nco*I fragment of the α3 gene. The construct (pGL3 control + 0.2 kb) was transfected in SY5Y neuroblastoma cells, and the resulting luciferase activity was compared with that determined by the wild-type pGL3 control. Only a very modest increase in the ability to drive the expression of the reporter gene was observed with pGL3 control + 0.2 kb [+30%, $F = 0.163$ (not statistically significant)] (Fig. 5), suggesting that the *Acc*III/*Nco*I region could properly work only in the context of the human α3 promoter, where its presence determined an increase in luciferase activity of 400% (Figs. 4 and 5). This result also made unlikely the hypothesis that the *Acc*III/*Nco*I fragment, being incorporated into the luciferase mRNA, could increase its stability or translation. Indeed, if the difference in luciferase activity between the 0.35 BN and the 0.16 BA human α3 promoter constructs (400%) had been due to a post-transcriptional effect of the *Acc*III/*Nco*I region, we could have reasonably expected a similar difference between pGL3 control and pGL3 control + 0.2 kb. On the other hand, it was possible that the functional properties of the *Acc*III/*Nco*I fragment relied on the ability to bind specific transcription factors; actually, this DNA region contains putative *cis*-acting elements for the transcription factors NFκB, AP-2, NF-1, and MED-1. To determine whether these putative *cis*-acting elements were functional, we carried out a mutation analysis (Fig. 5). Although a mutation in the NF-1 DNA site did not affect promoter activity (not shown), mutants in which the AP-2 or the NFκB putative binding sites were destroyed displayed a 50% decrease in the expression of the reporter gene. Therefore, we generated the construct ΔAP-2-ΔNFκB, with mutations in both sites. The plasmid showed a further 50% decrease in the promoter activity compared with the singly mutated parental plasmids, having a promoter strength identical to that of the 0.16-kb construct. These data indicated that the putative *cis*-acting elements for AP-2 and NFκB were actually functional and could account for the properties of the *Acc*III/*Nco*I fragment. However, we also identified in this fragment a recently discovered *cis*-acting element, MED-1, which has been shown to be common to many TATA-less, multistart site promoters (21). In the α3

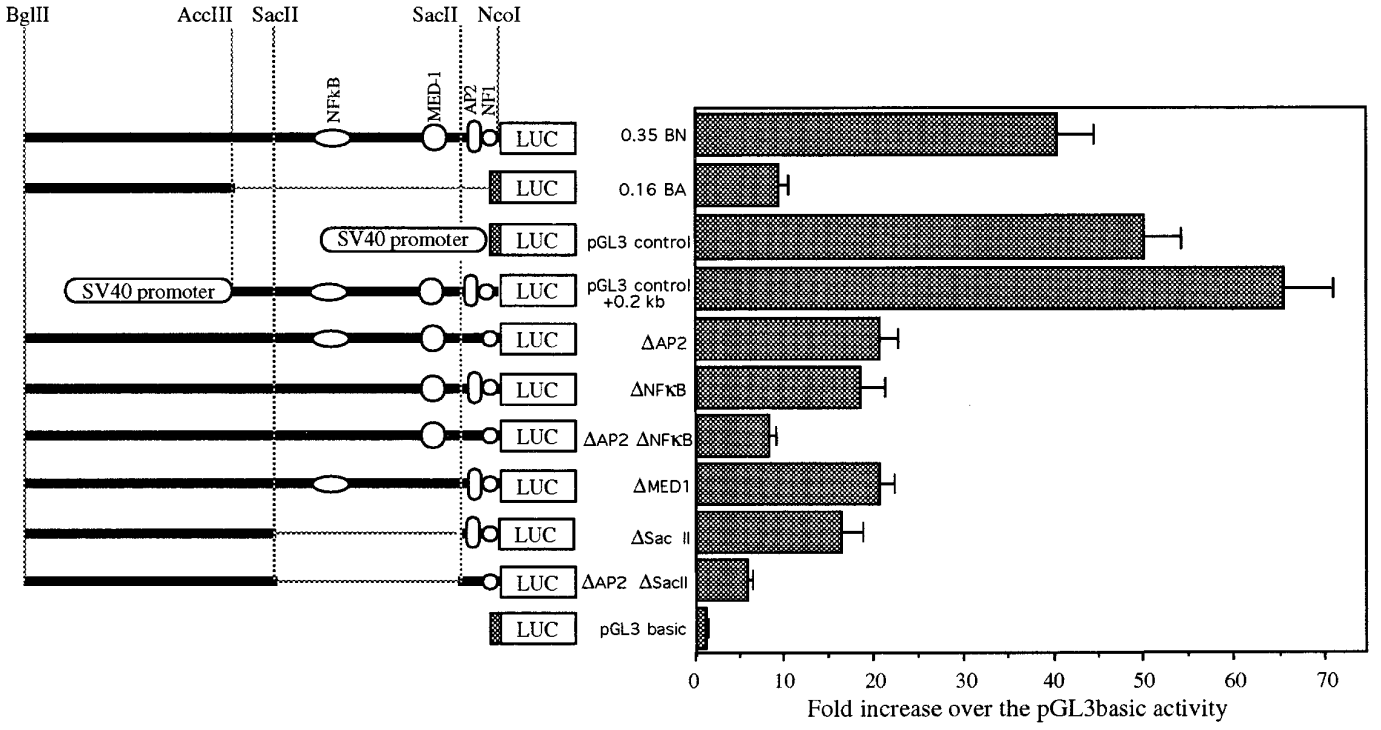

Fig. 5. Functional characterization of the *Acc*III/*Nco*I region in SY5Y cells. *Left*, scheme of the different constructs. The putative *cis*-acting elements for the indicated transcription factors are represented by specific symbols. The mutations of these elements are indicated by omitting the corresponding symbols in the specific construct. In the pGL3 control plasmid, the SV40 enhancer is located downstream of the luciferase (*LUC*) gene and is not indicated. *Bars*, transcriptional activity of the construct calculated as described in Materials and Methods and expressed as fold increase over the transcriptional activity of the promoterless plasmid pGL3-basic. The standard deviation is indicated. Each construct was tested at least three times in triplicate with two independent plasmid preparations. The difference in transcriptional activity between pGL3 control and pGL3 control + 0.2 kb was not statistically significant ($F = 0.163$) Differences in transcriptional activity between 0.35 BN and the mutated constructs, compared pairwise, were statistically significant ($F < 0.01$). Differences in transcriptional activity between 0.16 BA and the mutated constructs, compared pairwise, were statistically significant ($F < 0.05$) except the following pairs: 0.16 BA versus ΔAP-2-ΔNFκB and 0.16 BA versus ΔAP-2-Δ*Sac*II.

nicotinic subunit promoter, mutation of MED-1 determined a 50% decrease in the expression of the reporter gene (Fig. 5), confirming the functional role of this element in a novel TATA-less promoter. However, this finding also raised questions regarding the role of MED-1 in the context of the activity of the *Acc*III/*Nco*I downstream promoter region and of the functional correlations with AP-2 and NFκB. To approach these problems, we generated the Δ*Sac*II plasmid, in which both MED-1 and the putative NFκB *cis*-acting elements were removed. Δ*Sac*II displayed the same promoter strength as ΔMED-1 and ΔNFκB but without any further decrease in the expression of the reporter gene, as expected by the sum of the effects of the single mutations. When Δ*Sac*II was mutated in the downstream AP-2 putative binding site to obtain Δ*Sac*II-ΔAP-2, its transcriptional activity decreased by 50%, becoming similar to that of the 0.16 BA construct.

This finding suggested that the putative AP-2 binding site was able to carry out its function independent of the presence of the two other *cis*-acting elements.

Functional characterization of the 0.6 *Kpn*I/*Bgl*II region. The most relevant structural feature of the 0.6-kb *Kpn*I/*Bgl*II region is the presence of an Alu repeat (Fig. 1) in opposite orientation with regard to the direction of gene transcription that displays an 85% identity to the modern, primate-specific Alu consensus sequence described by Britten (22). Because Alu sequences have been shown to have regulatory functions on the activity of proximal promoters (23, 24), we decided to determine whether the α3 Alu repeat could account for the inhibitory influence of the 0.6-kb *Kpn*I/*Bgl*II region on gene expression (Fig. 6). For this reason, we generated the ΔAlu construct, in which most of the Alu repeat was removed. On transfection, the transcriptional activity of the construct seem to be increased by ~2.5-fold compared with that of the parental 1 KN plasmid, indicating that the deleted fragment significantly participates in the repression of the downstream promoter. Nevertheless, the ΔAlu construct does not possess the same promoter strength as the 0.35 BN plasmid. Because ΔAlu still contains the extremities of the Alu repeat and some outside flanking regions, we generated new constructs to test the influence of these sequences on α3 gene expression. The functional analysis of the 0.8 PN and 0.6 XN plasmids demonstrated that the region upstream of the Alu repeat, contained in the *Kpn*I/*Pst*I fragment, and the 5′ end of the Alu itself do not seem to play any relevant role in the inhibition of α3 gene expression. At the same time, it became clear that the element or elements responsible for the residual inhibitory activity on the downstream promoter should be contained either in the 3′ end of the Alu sequence or in the region between the *Ssp*I and *Bgl*II restriction sites. Interestingly, the 3′ end of the Alu repeat contains an element that was previously shown to work as a reducer in a monkey kidney fibroblast cell line (25). For this

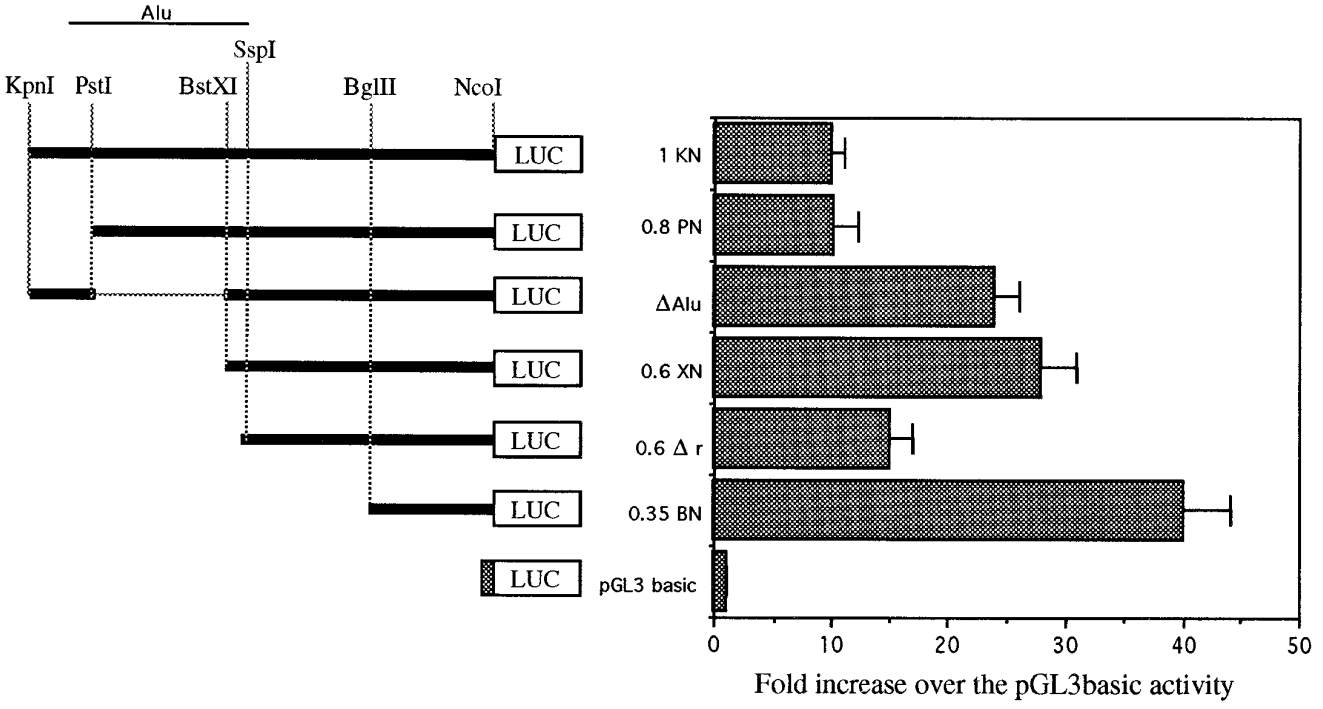

Fig. 6. Functional characterization of the 0.6-kb *Kpn*I/*Bgl*II region in SY5Y cells. *Left*, constructs; *top*, extent of the Alu sequence; *open box*, luciferase (*LUC*) gene coding region; *bars*, the transcriptional activity of the construct calculated as described in Materials and Methods and expressed as fold increase over the transcriptional activity of the promoterless plasmid pGL3-basic. The standard deviation is indicated. Each construct was tested at least three times in triplicate with two independent plasmid preparations. Differences in transcriptional activity between 0.35 BN and all other constructs, compared pairwise, were statistically significant ($F < 0.05$). Differences in transcriptional activity between 1 KN and all other constructs, compared pairwise, were statistically significant ($F < 0.05$) except the following pairs: 1 KN versus 0.8 PN and 1 KN versus 0.6 Δr.

reason, we generated the 0.6-kb Δr construct, in which in addition to the Alu sequence, the putative reducer element was removed. To our surprise, the transcriptional activity decreased by 50%, indicating that at least in our system, the reducer actually behaves as a positive element.

To summarize, these experiments demonstrate that the Alu repeat participates in the gene expression regulation of α3, working as a composite sequence in which at least one negative element and one positive element have been identified, located in the *Pst*I/*Bst*XI and *Bst*XI/*Ssp*I fragments, respectively. Furthermore, the region downstream of the Alu repeat, between the *Ssp*I and *Bgl*II restriction sites, still contains a *cis*-acting element or elements with relevant negative effects on the gene promoter activity.

Expression analysis of the human α3 nicotinic subunit 5′ regulatory region in non-neuronal cell lines. To understand the transcriptional mechanisms underlying the tissue-specific expression of the human α3 nicotinic subunit gene, we carried out transfection experiments in the non-neuronal cell lines TE671 and HeLa, which are not able to express the endogenous α3 subunit gene (Fig. 2A).

Fig. 7 shows a comparison of the transcriptional activities of the principal constructs in neuronal (SY5Y) and non-neuronal (TE671) cells. Similar results were obtained in HeLa cells (not shown). Although the 0.16 BA construct produced the same luciferase activity in both cell lines, the presence of the *Acc*III/*Nco*I fragment increased the expression of the reporter gene only in neuronal cells, as demonstrated by parallel transfections of the 0.35 BN construct. This represented an additional property of the previously characterized *Acc*III/*Nco*I region, whose positive influence on gene expression was exerted in a tissue-specific fashion. Also, the regulatory mechanisms of the 0.6-kb *Kpn*I/*Bgl*II fragment, which displayed an overall negative effect on the activity of the downstream promoter, seemed to be mainly operative in neuronal cells, with the paradoxical result that the 1 KN construct seemed to possess similar transcriptional activities in neuronal and non-neuronal cells.

Finally, we tested the entire β4–α3 intergenic region, showing that the 4.3 KN construct was four times less active in TE671 than in SY5Y. This different activity seems to be mainly due to the presence of positive element or elements in the 3.3-kb *Kpn*I/*Kpn*I fragment, which are functional in SY5Y, rather than to the presence of negative elements, which are functional in TE671.

Although our data indicate that positive elements of the α3 promoter are inefficient in non-neuronal cells, the residual transcriptional activity observed in TE671 and HeLa cells suggests that additional genetic mechanisms participate in the neural restricted expression of this nicotinic subunit gene.

Discussion

The α3 nicotinic subunit is abundantly expressed in the postganglionic neurons of vertebrates, including humans (26). All ganglion cells respond to preganglionic stimulation by a fast excitatory postsynaptic potential, which triggers the

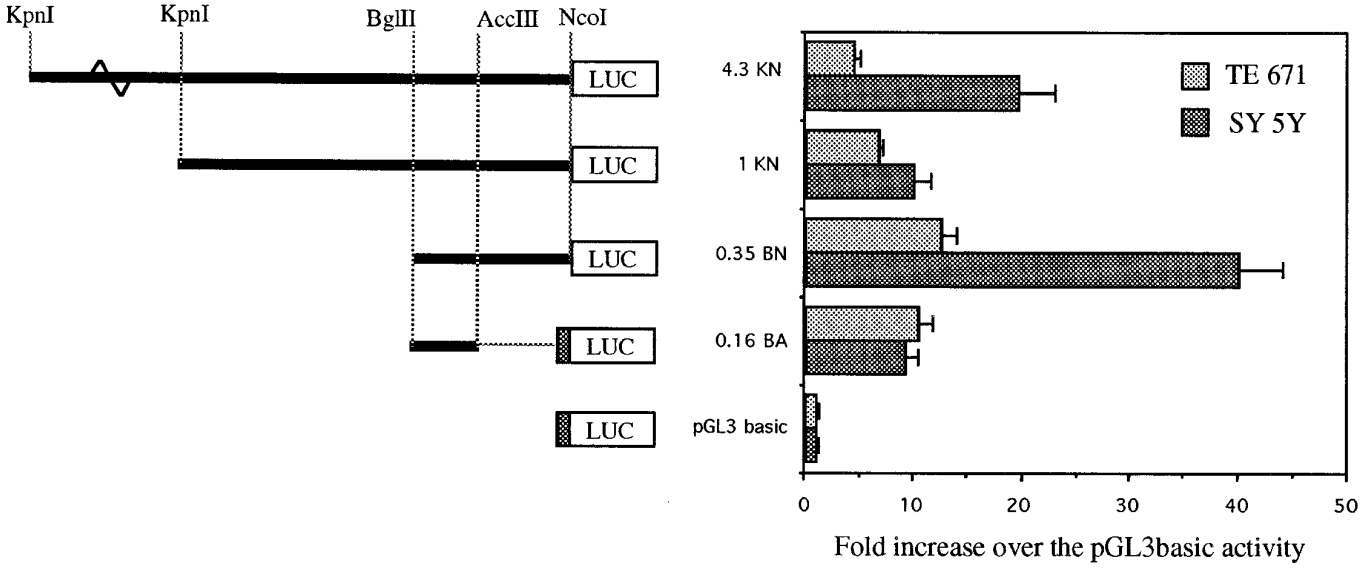

Fig. 7. Expression analysis of the human α3 nicotinic subunit 5′ regulatory region in non-neuronal cells. *Left*, chimeric constructs in which different parts of the α3 5′ regulatory region are fused to the luciferase (LUC) reporter gene. Note that the 3.3-kb *Kpn*I fragment is not to scale; *open box*, luciferase gene coding region; *shaded portion of the box*, DNA region specifying the 5′ UT of the luciferase. In the other constructs, the entire DNA region specifying the 5′ UT of the α3 mRNA was directly fused to the coding sequence of the reporter gene. *Bars*, transcriptional activity of the construct calculated as described in Materials and Methods and expressed as fold increase over the transcriptional activity of the promoterless plasmid pGL3-basic. The standard deviation is indicated. Each construct was tested at least three times in triplicate with two independent plasmid preparations.

initiation of the postsynaptic spike (27). The fast excitatory postsynaptic potential is due to the activation of nicotinic-acetylcholine receptors that contain α3 as essential agonist binding subunit (2).

The transcript encoding this subunit is also easily detectable in human neuroblastoma cell lines. Neuroblastomas are pediatric tumors that are thought to arise from migratory cells of the embryonal neural crest; several clonal cell lines have been stabilized from these tumors that display most of the features of the autonomic neurons, including the ability to express ganglionic-type nicotinic receptors (17, 18, 28). We exploited two human neuroblastoma cell lines, SY5Y and SK-N-BE, to characterize the gene promoter responsible for the expression of the human α3 nicotinic subunit gene.

To this purpose, we isolated a 4.3-kb *Kpn*I/*Nco*I fragment that corresponds to the genomic region contained between the coding sequences of the β4 and α3 genes.

RNase protection assays along with the functional dissection of this intergenic region allowed us to identify a 0.35-kb fragment immediately upstream of the start codon that was able to drive the expression of the luciferase reporter gene in both neuroblastoma cell lines with a strength comparable to that of the SV40 promoter/enhancer. The region displayed the features of a GC-rich, TATA-less, and CAAT-less promoter, with multiple transcription start points, located downstream of a series of putative Sp1 and AP-2 binding sites. In the past, TATA-less, CAAT-less multistart promoters were believed to be typical of housekeeping genes, but more recently it has become clear that the expression of neuron-specific genes can be driven by such a regulatory sequences.

In the current study, we focused on the downstream region of the human α3 promoter and the Alu sequence, upstream of the promoter; we also started to investigate the mechanisms responsible for the neurospecific expression of the α3 gene. Our results are discussed below.

Functional characterization of the downstream region of the human α3 promoter. The functional role of *cis*-acting elements located downstream of the transcription start point and incorporated into the mature transcript has been reported (13, 28). In a recent report, the region downstream of the human immunodeficiency virus type 1 promoter, which specifies the gag leader sequence, was proved to contain some putative *cis*-acting elements, whose mutations severely affected gene transcription (29). The *Acc*III/*Nco*I region contains putative *cis*-acting elements for the transcription factors AP-2 and NFκB. AP-2 has been shown to be expressed in cells derived from the neural crest (30), including the postganglionic neurons. NFκB actually identifies a family of inducible transcription factors with a wide range of activities in different tissues (31). Although in many tissues the first step of the NFκB activation from different external stimuli is the translocation of the factor from the cytoplasm to nucleus, in neuronal cells some members of the family can be constitutively localized in the nucleus (32), where they likely participate in the regulation of the expression of the target genes. Notably, both NFκB and AP-2 DNA binding activities have been documented in unstimulated SY5Y nuclear extracts (33, 34). Although the molecular identity of the transcription factors that bind to the DNA consensus motifs in the *Acc*III/*Nco*I region remains to be confirmed, we showed that a double mutation in the AP-2 and NFκB putative *cis*-acting elements reduces by 4-fold the transcriptional activity of the 0.35 BN construct, bringing it down to the level of that of the 0.16 BA construct. Thus, the two putative *cis*-acting elements not only are functional but also could account for the entire activity of the *Acc*III/*Nco*I region. However, it is likely that the molecular mechanisms that take place in the

context of the *Acc*III/*Nco*I region are more complex than the simple sum of the positive activities of two transcription factors. We reached this conclusion by exploring the functional role of a novel *cis*-acting element, MED-1, that has been shown to be common to many TATA-less, multistart site promoters (21). In the *pgp1* promoter, the element is able to bind a nuclear protein, as demonstrated by gel shift analysis, and its mutation was proved to reduce the expression to 25% of that of the wild-type promoter. The element and its cognate protein might act as selectors or activators of multiple start sites and regulate them as a cassette rather than individually. However, the precise molecular mechanism underlying the functional role of MED-1 is not yet known.

In the human α3 promoter, mutation of MED-1 determined a 50% decrease in the promoter strength, suggesting a participation of the site in the activity of the *Acc*III/*Nco*I fragment.

The same reduction was also detected by mutating the NFκB putative *cis*-acting element alone. To our surprise, no further decrease in gene expression was observed when both MED-1 and NFκB sites were deleted in the Δ*Sac*II construct, as if the two factors did not work independently but rather influenced each other in the ability to regulate gene expression. This is in line with the suggestion of Ince and Scotto (21), who proposed that "MED-1 is necessary but not sufficient for multiple start site utilization and that other, likely *trans*-acting, factor/s impose a higher order of regulation on the recognition of this element." On the contrary, the downstream AP-2 *cis*–acting element seems to influence promoter activity autonomously; indeed, mutation of this site always produced a 50% decrease in the expression of the reporter gene.

The activity of the *Acc*III/*Nco*I region seems to be dependent on the cellular and promoter contexts in which it is placed. Indeed, the presence of this region does not affect the expression of the reporter gene in non-neuronal cells and only modestly increases the expression of the luciferase in neuronal cells when placed downstream of the SV40 early promoter. A restricted interaction between a tissue-specific regulatory element and the natural core promoter has been demonstrated for the human myoglobin gene (35), in which the muscle-specific enhancer is able to work in conjunction with the core promoter elements of the myoglobin gene but not in combination with the SV40 early promoter.

Altogether, our data are consistent with the hypothesis that the enhancing activity of the *Acc*III/*Nco*I region relies on transcriptional mechanisms but does not definitively rule out the possible role of post-transcriptional effects on the translatability or stability of the mRNA.

An Alu sequence, upstream of the α3 promoter, participates in gene expression regulation. Alu sequences are transposable elements specific to primates that by moving into positions of significance to gene expression are believed to be a source of evolutionary change (36). In particular, Alu sequences have been shown to have regulatory functions when located near promoters, with either positive or negative effects on gene expression (23, 24). Our data are in line with this evidence, demonstrating that the α3 Alu repeat behaves as a composite region in which positive and negative elements coexist. Surprisingly, the positive element corresponds to a DNA sequence of the Alu repeat previously characterized as a "reducer" in monkey kidney fibroblast cell lines CV-1 and COS-1 (25).

The negative effects of the remaining part of the Alu repeat could be due, according to the literature, to transcriptional interference or direct inhibition of proximal promoters. Transcriptional interference relies on the presence in the Alu sequence of a RNA polymerase III promoter whose activity can reduce the transcription from a nearby polymerase II promoter (24, 37). The Alu sequence upstream of the α3 promoter shows an almost complete deletion of the *Pol*III promoter, excluding the possibility of transcriptional interference. Direct inhibition relies on the negative effects of transcription factors bound to *cis*-acting elements within the Alu sequences. Two different types of negative *cis*-acting elements have been identified in Alu repeats: a 38-bp "reducer element" and the sequence motif GGAGGC (also known as Alu core) (25, 38). The α3 Alu sequence contains two "reducer elements" (one of them actually works as activator, as previously described) and three copies of the Alu core. Furthermore, it is possible that additional reducer-like sequences have evolved in the context of the α3 Alu repeat.

The functional dissection of the *Kpn*I/*Bgl*II fragment also revealed that the region immediately downstream of the Alu repeat (*Ssp*I/*Bgl*II fragment) contains negative element or elements that keep the reporter gene expression down by ~3-fold, adding further complexity to the mechanisms that govern the transcription of the human α3 gene.

The 5′ regulatory sequences of the α3 gene drive the expression of the reporter gene preferentially, but not exclusively, in neuronal cells. In humans, as in other species, the expression of the α3 nicotinic subunit has been demonstrated by *in situ* hybridization in the CNS (39), autonomic ganglia (26), and adrenal medulla.[2] In the current study, we analyzed the behavior of some constructs in non-neuronal cells, with the aim of understanding whether the β4–α3 intergenic region contained the elements responsible for the restricted expression of the α3 subunit. We used Hela cells (data not shown) and TE671, a rhabdomyosarcoma cell line that is able to express muscle-type but not neuronal-type nicotinic receptors. Although the 4.3 KN construct displayed a preferential neurospecific expression pattern and some DNA regions were proved to work preferentially or exclusively in neuroblastoma cells, we could not demonstrate a completely neurospecific activity of the human α3 5′ flanking region; there are several possible explanations. In the past few years, an NRSE and its cognate *trans*-acting factor, neuron restrictive silencer factor/RE1-silencing transcription factor, have been identified that are able to switch off the expression of neurospecific genes in non-neuronal cells (for a review, see Ref. 40). It is possible that we missed an NRSE because it is located outside of the β4–α3 intergenic region. Interestingly, an NRSE was recently identified and proved to be functional in the mouse β2 nicotinic subunit promoter (13). It is also possible that tissue-specific DNA modifications, such as methylation, or proper interactions with chromatin are needed to reach a full neurospecific activity of the α3 regulatory region. These issues, which cannot be addressed with transient transfection experiments, are under study through the generation of stable transfectants.

Some differences in the α3 gene expression regulation were

[2] M. Mandelli, personal communication.

also detected between the neuroblastoma cell lines. In the SK-N-BE cells, the regulatory effects of the 3.3-kb *Kpn*I fragment on α3 gene expression were apparently absent, whereas in SY5Y cells, the deletion of this region produced a 50% decrease in the expression of the reporter gene. Furthermore, the two cell lines displayed different uses of the same transcription start sites and expressed different levels of α3 transcript. Although we do not have a definitive explanation for these differences, we speculate that this diversity in the expression and in the regulation of the α3 mRNA may reflect a different differentiation stage of the two cell lines.

The genetic mechanisms responsible for the expression of the rat α3 nicotinic subunit (8–11) have been characterized by different groups. They demonstrated, also in this species, that the transcription of the gene is driven by a GC-rich, multistart site promoter with no TATA or CAAT box. Molecular characterization of the minimal promoter revealed that an Sp1 consensus motif plays a relevant role in the expression of the gene in PC12, whereas an AP-2 binding site may not have any function (11). This may represent an important difference from the human promoter. Unfortunately, no characterization of the segment specifying the 5′ UT region has been carried out, so it is not possible to establish whether it plays a similar role as the human counterpart. The rat genome does not contain Alu sequences. Furthermore, no regulatory activities have been demonstrated in the region immediately upstream of the rat α3 nicotinic subunit promoter. Therefore, our data suggest that the human α3 gene has acquired novel transcriptional control mechanisms during evolution and indicate that despite an high homology in terms of coding regions, important differences in the regulatory sequences, with functional implications, may exist across species.

Acknowledgments

We are very grateful to Dr. Nica Borgese for critical revision of the manuscript and to Dr. Marco Righi for his help in computer-assisted analysis. We thank Mr. Paolo Tinelli for the photography.

References

1. Sargent, P. B. The diversity of neuronal nicotinic acetylcholine receptors. *Annu. Rev. Neurosci.* **16:**403–443 (1993).
2. McGehee, D. S., and L. Role. Physiological diversity of nicotinic acetylcholine receptors expressed by vertebrate neurons. *Annu. Rev. Physiol.* **57:** 521–546 (1995).
3. Ramirez-Latorre, J., C. R. Yu, X. Qu, F. Perin, A. Karlin, and L. Role. Functional contributions of α5 subunit to neuronal acetylcholine receptor channels. *Nature (Lond.)* **380:**347–351 (1996).
4. Wada, E., K. Wada, J. Boulter, E. Deneris, S. Heinemann, J. Patrick, and L. W. Swanson. Distribution of α2, α3, α4 and β2 neuronal nicotinic receptor subunit mRNA in the central nervous system: a hybridization histochemical study in the rat. *J. Comp. Neurol.* **284:**314–335 (1989).
5. Zoli, M., N. Le Novere, J. A. Hill, and J. P. Changeux. Developmental regulation of nicotinic Ach receptor subunit mRNA in the rat central and peripheral nervous system. *J. Neurosci.* **15:**1912–1939 (1995).
6. Cimino, M., P. Marini, S. Colombo, M. Andena, F. Cattabeni, D. Fornasari, and F. Clementi. Expression of neuronal acetylcholine nicotinic receptor α4 and β2 subunits during postnatal development of the rat brain. *J. Neural. Transm.* **100:**77–92 (1995).
7. Matter-Sadzinski, L., M. C. Hernandez, T. Roztocil, M. Ballivet, and J. M. Matter. Neuronal specificity of the α7 nicotinic acetylcholine receptor promoter develops during morphogenesis of the central nervous system. *EMBO J.* **11:**4529–4538 (1992).
8. Duvoisin, R. M., and S. Heinemann. Transcription control elements of the rat neuronal nicotinic acetylcholine receptor subunit α3. *Braz. J. Med. Biol. Res.* **26:**137–150 (1993).
9. Yang, X., J. McDonough, D. Fyodorov, M. Morris, F. Wang, and E. S. Deneris. Characterization of an acetylcholine receptor α3 gene promoter and its activation by the POU domain factor Scip/Tst-1. *J. Biol. Chem.* **269:**10252–10264 (1994).
10. R. T. Boyd. Sequencing and promoter analysis of the genomic region between the rat neuronal nicotinic acetylcholine receptor *beta* 4 and *alpha* 3 genes. *J. Neurobiol.* **25:**960–973 (1994).
11. Yang, X., D. Fyodorov, and E. S. Deneris. Transcriptional analysis of acetylcholine receptor *alpha* 3 gene promoter motifs that bind Sp1 and AP-2. *J. Biol. Chem.* **270:**8514–8520 ((1995).
12. Milton, N. G., A. Bessis, J. P. Changeux, and D. S. Latchman. The neuronal nicotinic acetylcholine receptor *alpha* 2 subunit gene promoter is activated by the Brn-3b POU family transcription factor and not by Brn-3a or Brn-3c. *J. Biol. Chem.* **270:**15143–15147 (1995).
13. Bessis, A., A. M. Salmon, M. Zoli, N. Le Novere, M. Picciotto, and J. P. Changeux. Promoter elements conferring neuron-specific expression of the *beta* 2 subunit of the neuronal nicotinic acetylcholine receptor studied in vitro and in transgenic mice. *Neuroscience* **69:**807–819 (1995).
14. Hu, M., N. L. Whiting Theobald, and P. D. Gardner. Nerve growth factor increases the transcriptional activity of the rat neuronal nicotinic acetylcholine receptor β4 subunit promoter in transfected PC12 cells. *J. Neurochem.* **62:**392–395 (1994).
15. Hernandez, M. C., L. Erkman, L. Matter-Sadzinski, T. Roztocil, M. Ballivet, and J. M. Matter. Characterization of the nicotinic acetylcholine receptor β3 gene. *J. Biol Chem.* **270:**3224–3233 (1995).
16. Raimondi, E., F. Rubboli, D. Moralli, B. Chini, D. Fornasari, P. Tarroni, L. De Carli, and F. Clementi. Chromosomal localization and physical linkage of the genes encoding the human α3, α5, and β4 neuronal nicotinic receptor subunits. *Genomics* **12:**849–850 (1992).
17. Tarroni, P., F. Rubboli, B. Chini, R. Zwart, M. Oortgiesen, E. Sher, and F. Clementi. Neuronal-type nicotinic receptors in human neuroblastoma and small-cell lung carcinoma cell lines. *FEBS* **312:**66–70 (1992).
18. Fornasari, D., B. Chini, P. Tarroni, and F. Clementi. Molecular cloning of human neuronal nicotinic receptor α3 subunit. *Neurosci. Lett.* **111:**351–356 (1990).
19. Young, D. C., S. D. Kingsley, K. A. Ryan, and F. J. Dutko. Selective inactivation of eukaryotic β-galactosidase in assays for inhibitors of HIV-1 TAT using bacterial β-galactosidase as a reporter gene. *Anal. Biochem.* **215:**24–30.
20. M. Kozak. An analysis of vertebrate mRNA sequences: intimations of translational control. *J. Cell Biol.* **115:**887–903 (1991).
21. Ince, T. A., and K. W. Scotto. A conserved downstream element defines a new class of RNA polymerase II promoters. *J. Biol. Chem.* **270:**30249–30252 (1995).
22. R. J. Britten. Evolutionary selection against change in many Alu repeat sequences interspersed through primate genomes. *Proc. Natl. Acad Sci. USA* **91:**5992–5996 (1994).
23. Hambor, J. E., J. Mennone, M. E. Coon, J. H. Hanke, and P. Kavathas. Identification and characterization of an Alu-containing, T-cell specific enhancer located in the last intron of the human CD8α gene. *Mol. Cell. Biol.* **13:**7056–7070 (1993).
24. Wu, J., G. J. Grindlay, P. Bushel, L. Mendelsohn, and M. Alan. Negative regulation of the human ϵ-globin gene by transcriptional interference: role of an Alu repetitive element. *Mol. Cell. Biol.* **10:**1209–1216 (1990).
25. Saffer, J. D., and S. J. Thurston. A negative regulatory element with properties similar to those of enhancers is contained within an Alu sequence. *Mol. Cell. Biol.* **9:**355–364 (1989).
26. Cimino M., P. Marini, D. Fornasari, F. Cattabeni, and F. Clementi. Distribution of nicotinic receptors in Cynomolgus monkey brain and ganglia: localization of α3 subunit mRNA, α-bungarotoxin and nicotine binding sites. *Neuroscience* **51:**77–86 (1992).
27. A. A. Selyanko. Properties of nicotinic postsynaptic receptor channels in ganglia, in *Autonomic Ganglia* (E. M. McLachlan, ed.). Autonomic Nervous System Series Vol. 6. Harwood Academic Publishers, Chur, Switzerland 213–258 (1995).
28. Mariman, E., and B. Wieringa. Expression of the gene encoding human brain creatinine kinase depends on sequences immediately following the transcription start point. *Gene* **102:**205–212 (1991).
29. El Kharroubi, A., and M. A. Martin. *cis*-acting sequences located downstream of the human immunodeficiency virus type 1 promoter affect its chromatin structure and transcriptional activity. *Mol. Cell. Biol.* **16:**2958–2966 (1996).
30. Mitchell, P. J., P. M. Timmons, J. M. Hebert, P. W. J Rigby, and R. Tjian. Transcription factor AP-2 is expressed in neural crest cell lineages during mouse embryogenesis. *Genes. Dev.* **5:**105–119 (1991).
31. Grilli, M. G., J. J. S. Chiu, and M. J. Lenardo. NFκB and Rel: participants in a multiform transcriptional regulatory system. *Int. Rev. Cytol.* **143:**1–62 (1993).
32. Kaltschmidt, C., B. Kaltschmidt, H. Neumann, H. Wekerle, and P. A. Baeuerle. Constitutive NF-*kappa* B activity in neurons. *Mol. Cell. Biol.* **14:**3981–3992 (1994).
33. Grilli, M., F. Goffi, M. Memo, and P. F. Spano. Interleukin-1β and glutamate activate the NFκB/Rel binding site from the regulatory region of the amyloid precursor protein gene in primary neuronal culture. *J. Biol. Chem.* **271:**15002–15007 (1996).
34. Greco, D., E. Zellmer, Z. Zhang, and E. Lewis. Transcription factor AP-2 regulates expression of the dopamine *beta*-hydroxylase gene. *J. Neurochem.* **65:**510–516 (1995).

35. Wefald, F. C., B. H. Devlin, and R. S. William. Functional heterogeneity of mammalian TATA-box sequences revealed by interaction with a cell-specific enhancer. *Nature (Lond.)* **344:**260–262 (1990).
36. J. F. McDonald. Evolution and consequences of transposable elements. *Curr. Opin. Genet. Dev.* **3:**855–864 (1993).
37. Hull, M. W., J. Erickson, M. Johnston, and D. R. Engelke. tRNA genes as transcriptional repressors elements. *Mol. Cell. Biol.* **14:**1266–1277 (1994).
38. Tomilin, N. V., S. M. M. Iguchi-Ariga, and H. Ariga. Transcription and replication silencer element is present within conserved region of human Alu repeats interacting with nuclear protein. *FEBS* **263:**69–72 (1990).
39. Rubboli, F., J. A. Court, C. Sala, C. Morris, B. Chini, E. Perry, and F. Clementi. Distribution of nicotinic receptors in the human hippocampus and thalamus. *Eur. J. Neurosci.* **6:**1596–1604 (1994).
40. Schoenherr, C. J., and D. J. Anderson. Silencing is golden: negative regulation in the control of neuronal gene transcription. *Curr. Opin. Neurobiol.* **5:**566–571 (1995).

Send reprint requests to: Dr. Diego Fornasari, CNR Cellular and Molecular Pharmacology Center, Department of Medical Pharmacology, University of Milan, Via Vanvitelli 32, 20129 Milan, Italy. E-mail: diegof@farma9.csfic.mi.cnr.it